

Supplementary Material

for

Structural and Functional Analysis of *Campylobacter jejuni* PseG: A UDP-Sugar Hydrolase from the Pseudaminic Acid Biosynthetic Pathway

Erumbi S. Rangarajan[‡], Ariane Proteau[§], Qizhi Cui[§], Susan M. Logan[¶], Zhanna Potetinova[¶], Dennis Whitfield[¶], Enrico O. Purisima[§], Mirosław Cygler^{§‡}, Allan Matte[§], Traian Sulea^{§*}, and Ian C. Schoenhofen^{¶*}

From the [‡]Department of Biochemistry, McGill University, Montreal, QC Canada, the [§]Biotechnology Research Institute, National Research Council of Canada, 6100 Royalmount Ave., Montreal, QC H4P 2R2 Canada, and the [¶]Institute for Biological Sciences, National Research Council of Canada, 100 Sussex Drive, Ottawa, ON K1A 0R6 Canada

* To whom correspondence may be addressed, ICS: ian.schoenhofen@nrc-cnrc.gc.ca, 613-991-2141 (tel), 613-952-9092 (fax), or TS: traian.sulea@nrc-cnrc.gc.ca, 514-496-1924 (tel), 514-496-5143 (fax).

Table S1. Mutagenic oligonucleotides used in this study.

Oligonucleotide	Sequence (5'→3')
H17F-F H17F-R	GCTCCAGTCAAATAGGCTTTGGATT TT CATTAAACGCGATCTAGTCTTAGC GCTAAGACTAGATCGCGTTTAATG AA TCCAAAGCCTATTTGACTGGAGC
H17L-F H17L-R	GCTCCAGTCAAATAGGCTTTGGACT T CATTAAACGCGATCTAGTCTTAGC GCTAAGACTAGATCGCGTTTAATG AG TCCAAAGCCTATTTGACTGGAGC
H17N-F H17N-R	GCTCCAGTCAAATAGGCTTTGGAA A CATTAAACGCGATCTAGTCTTAGC GCTAAGACTAGATCGCGTTTAATGT T TCCAAAGCCTATTTGACTGGAGC
Y78F-F Y78F-R	GAACTTCTTATCATTGATCACT TC GGCATCAGCGTAGATGATGAAAACTG CAGTTTTTCATCATCTACGCTGATGCC GA AGTGATCAATGATAAGAAGTTC
N255A-F N255A-R	GGCAAATTTCAAAGCTATTTGTTATGTTAAAG GC TCAAGAATCTACAGCAACTTGGCTTGC GCAAGCCAAGTTGCTGTAGATTCTTGAG GC TTTAACATAACAAATAGCTTTGAAATTTGCC

Table S2. α -helical parameters for PseG variants obtained from CD experiments (see Fig. S2 for further details).

PseG or variant	MW	[c] mg/ml	ABS ₂₈₀	$-[\theta] \times 10^{-3}$ (λ_{\min} , nm)	$-[\theta]_{209} \times 10^{-3}$	$-[\theta]_{222} \times 10^{-3}$	$[\theta]_{222}/[\theta]_{209}$
17.1	32383.3	0.099	0.082	11.22 (213.6)	9.55	8.69	0.91
133.1	32384.2	0.102	0.084	12.20 (212.2)	11.01	9.32	0.85
N255A	32340.3	0.100	0.083	11.61 (212.8)	10.43	8.94	0.86
17.1(2)	32383.3	0.098	0.081	10.94 (213.2)	9.61	8.37	0.87
H17L	32359.3	0.099	0.082	10.84 (210.8)	10.56	8.22	0.78
H17N	32360.2	0.098	0.081	11.32 (212.0)	10.29	8.04	0.78
H17F	32393.3	0.101	0.083	11.72 (213.4)	9.52	8.81	0.93
Y78F	32367.3	0.104	0.081	9.57 (212.0)	8.87	7.01	0.79

$\epsilon_{280}=26735 \text{ M}^{-1}\text{cm}^{-1}$ (for all compounds except only Y78F)

$\epsilon_{280}=25245 \text{ M}^{-1}\text{cm}^{-1}$ (for Y78F)

cell length: 0.05 cm

Table S3. PseG-substrate solvated interaction energy (SIE) and PseG solvated conformational energy (SCE) for predicted models for PseG-substrate complexes corresponding to 5S_1 and 1C_4 sugar ring conformations of the substrate.

Energy (kcal/mol)	PseG-UDP-(5S_1)- 6-deoxy-AltdiNAc	PseG-UDP-(1C_4)- 6-deoxy-AltdiNAc
$\langle E_C \rangle^a$	-61.51 ± 0.51	-58.12 ± 0.52
$\langle E_{vdw} \rangle$	-75.07 ± 0.33	-72.84 ± 0.27
$\langle \gamma \cdot \Delta MSA \rangle$	-13.84 ± 0.02	-12.93 ± 0.03
$\langle \Delta G_{bind}^R \rangle$	46.99 ± 0.32	56.77 ± 0.32
$\langle SIE \rangle_{PseG-substrate}^b$	-13.72 ± 0.04	-12.02 ± 0.05
$\langle SCE \rangle_{PseG}^c$	116.05 ± 0.38	127.28 ± 0.37

^a $\langle \dots \rangle$ denotes the average over 160 snapshots at 0.5 ps intervals from the last 80 ps QM/MM MD trajectory of the complex after solvent and ions were stripped off. The uncertainties are mean standard errors.

$${}^b SIE(\rho, D_{in}, \alpha, \gamma, C) = \alpha \cdot [E_C(D_{in}) + \Delta G_{bind}^R(\rho, D_{in}) + E_{vdw} + \gamma \cdot \Delta MSA(\rho)] + C$$

represents intermolecular (protein-ligand) solvated interaction energy, where E_C and E_{vdw} are the intermolecular Coulomb and van der Waals interaction energies in the bound state, respectively, calculated using the AMBER molecular mechanics force field with an optimized dielectric constant. The ΔG_{bind}^R is the change in the reaction field energy between the bound and free states, calculated by solving the Poisson equation with the boundary element method program, BRI BEM (1,2) and using a molecular surface generated with a variable-radius solvent probe (3). The free (uncomplexed) state is approximated by rigid separation from the complex. The ΔMSA term is the change in molecular surface area upon binding. The AMBER van der Waals radii linear scaling coefficient (ρ), the solute interior dielectric constant (D_{in}), the molecular surface area coefficient (γ), the global proportionality coefficient relating to the loss of configurational entropy upon binding (α), and a constant (C), are parameters calibrated by fitting

to the absolute binding free energies for a set of 99 protein-ligand complexes (4). The optimized values of these parameters are $\alpha = 0.1048$, $D_{\text{in}} = 2.25$, $\rho = 1.1$, $\gamma = 0.0129$ kcal/mol/Å², and $C = -2.89$ kcal/mol.

$${}^{\circ} \text{SCE}(\rho, D_{\text{in}}, \alpha, \gamma) = \alpha \cdot [E_{\text{bond}} + E_{\text{angle}} + E_{\text{torsion}} + E_{\text{improper}} + E_{\text{vdW14}} + E_{\text{vdW15}} + E_{\text{elec14}} + E_{\text{elec15}} + G^{\text{R}}(\rho, D_{\text{in}}) + \gamma \cdot \Delta \text{MSA}(\rho)]$$

represents the solvated conformational energy of a solute, where, E_{bond} , E_{angle} , E_{torsion} , E_{improper} , E_{vdW14} , E_{vdW15} , E_{elec14} , and E_{elec15} are intramolecular energy terms calculated with the AMBER force field, $G^{\text{R}}(\rho, D_{\text{in}})$ is the reaction field energy calculated with BRI BEM (1,2) using a molecular surface generated with a variable-radius solvent probe (3), and MSA is the molecular surface area. The parameters α , ρ , D_{in} and γ take the same values as for the SIE calculation. Here, SCE of the protein (PseG) was calculated for its substrate-bound conformation after rigid extraction from the complex.

References

1. Purisima, E. O. (1998) *J. Comput. Chem.* **19**, 1494-1504.
2. Purisima, E. O., and Nilar, S. H. (1995) *J. Comput. Chem.* **16**, 681-689.
3. Bhat, S., and Purisima, E. O. (2006) *Proteins* **62**, 244-261.
4. Naim, M., Bhat, S., Rankin, K. N., Dennis, S., Chowdhury, S. F., Siddiqi, I., Drabik, P., Sulea, T., Bayly, C. I., Jakalian, A., and Purisima, E. O. (2007) *J. Chem. Inf. Model.* **47**, 122-133.

Supplemental Figure Legends

Fig. S1. SDS-PAGE (12.5%) analyses of *C. jejuni* PseGHis₆ derivatives after nickel-nitrilotriacetic acid purification, 1 µg each. Lane 1, WT; lane 2, H17F; lane 3, H17L; lane 4, H17N; lane 5, Y78F; lane 6, N255A. Molecular mass standards are shown on the left in kDa.

Fig. S2. CD spectra for PseGHis₆ and variants. (A) 17.1 (WT E155K), 133.1 (WT) and N255A (E155K) as well as (B) 17.1 (WT E155K), H17L (E155K), H17N (E155K), H17F (E155K) and Y78F (E155K) in 25 mM sodium phosphate pH 7.3, 25 mM NaCl. Protein concentrations were 0.098 - 0.104 mg/ml. CD α -helix parameters are shown in Table S2.

Fig. S3. Optimized conformations of the free 6-deoxy-AltdiNAc sugar (O1-methylated) from DFT QM calculations. Assigned ring conformations according to Berces *et al.* (Berces, A., Nukada, T., and Whitfield, D. M. (2001) *Tetrahedron* **57**, 477-491).

Fig. S4. Identification of critical residues in the putative PseG hydrolase family. Multiple sequence alignment of several PseG representatives carried out using MUSCLE (Edgar, R. C. (2004) *BMC Bioinformatics* **5**, 113). The PseG and related sequences used are from *Campylobacter jejuni* (gi15792635), *Helicobacter pylori* (HP0326B), *Aeromonas punctata* (gi5616173), *Aeromonas hydrophila* (gi74273852), *Pseudomonas aeruginosa* (gi20560143 and gi20560095), *Rhizobium* species NGR234 (gi86772969) and *Sinorhizobium meliloti* (gi6523008). The sequence of the structurally related *Escherichia coli* MurG glycosyltransferase is also aligned based on structural superpositions of its substrate-bound crystal structure (PDB code 1NLM, molecule A) onto the UDP-bound *C. jejuni* PseG crystal structure (this work). Invariant residues within the PseG hydrolase family are highlighted on a red background, including those that are conserved in MurG. Observed secondary structure elements (arrows: β -strands; cylinders: α -helices) are indicated above the *C. jejuni* PseG sequence and below the *E. coli* MurG sequence. Residues within 4 Å from the UDP moiety in the two

structures are indicated with green dots, those within 4 Å from the respective donor sugar moieties are marked by blue triangles. These residues are further labeled according to their participation in interactions with the substrate *via* their main-chain (m) side-chain (s), or both (b). Note that residue numbering of *E.coli* MurG differs by 1 in its crystal structure (PDB code 1NLM) relative to the Swiss-Prot entry (P17443), due to an additional methionine at the N-terminus in the crystal structure. In order to provide a streamlined structural comparison, we adopted the crystal structure numbering of *E.coli* MurG throughout this paper.

Fig. S5. Ligand binding in the inter-domain tunnel of PseG. (A) Overall view of PseG represented as a Z-sliced molecular surface (magenta) on the left and as a main-chain ribbon with secondary structure elements (spectrum colored from N-terminus – blue to C-terminus – red) on the right. Close-up views in the tunnel reveal (B) the bound UDP, glycerol and water molecules from the crystal structure, and (C) the UDP-6-deoxy-AltdiNAc substrate from the modeled structure (the 2N acetyl group is cut-out from the view by Z-slicing).

Fig. S6. Analysis of QM/MM MD trajectories for PseG-substrate complexes with the sugar ring in the 1C_4 (red curve) and 5S_1 (black curve) conformations. (A) Sugar ring stability expressed as the τ_5 dihedral angle (C2-C1-O5-C5), (B) distance between the anomeric C1 atom of the sugar ring and the NE atom of His17, (C) partial charge on the anomeric C1 atom, (D) partial charge on the anomeric O_{gly} atom, (E) substrate-induced RMS deviations in the PseG active site region (Q12-H17, K19, R20, Y78, D101, N115, R143, F146, C163-I169, A189, T190, I219, S232-L236, E239, Y252, V253, N255, Q256, T259) from the crystal structure of the PseG-UDP complex, and (F) flexibility of the substrate-complexed PseG expressed as time- and residue-averaged RMS fluctuations, with residues in the active site region (indicated above) highlighted by filled circles.

Fig. S7. Water structure around the PseG-substrate complex calculated from the QM/MM MD simulations. The model with the sugar ring of the substrate in 5S_1 conformation is

shown in (A), and the model in 1C_4 conformation is shown in (B). Water occupancy is indicated as density contours represented by solid isosurfaces colored red for water oxygen atoms and white for water hydrogen atoms. Contours are drawn at 25% of the maximal density values for the water O and H atoms. The density plots are calculated on a 0.2 Å spaced Cartesian cubic grid (40 x 40 x 40 Å) centered on the center of mass of the substrate. The calculations were done on the last 120 ps and 90 ps of QM/MM MD simulations for the models corresponding to the 5S_1 and 1C_4 sugar ring conformations, respectively. The shown coordinates of the solutes (PseG and substrate) are averaged (not energy minimized) over the same simulation window. An arrow indicates the calculated location of the putative nucleophilic water O atom. Select PseG side-chains are shown and labeled (for Ile13 the main-chain carbonyl group is rendered). The viewing orientations are similar to those in Fig. 4AB of the main paper. Figure produced using VMD 1.8.5 (Humphrey, W., Dalke, A., and Schulten, K. (1996) *J. Mol. Graphics* **14**, 33-38).

Fig. S8. Kinetic analysis of PseGHis₆ and respective substitution derivatives. Michaelis-Menten and Eadie-Hofstee (*insets*) analysis of PseG (A), PseG Y78F (B), PseG H17N (C) and PseG N255A (D) reactions with the substrate UDP-2,4-diacetamido-2,4,6-trideoxy-β-L-altropyranose.

Fig. S9. Structural comparison of PseG-UDP-6-deoxy-AltdiNAc (yellow) and MurG-UDP-GlcNAc (magenta) complexes based on (A) an RMS fit of protein Cα atoms, and (B) an RMS fit of the UDP moiety of the substrates plus Cα atoms from select residues from the core β-sheet of the C-terminal domain of the proteins. The side chains of the putative catalytic residue His17 of PseG and of the corresponding conserved residue in MurG (His19) are highlighted.

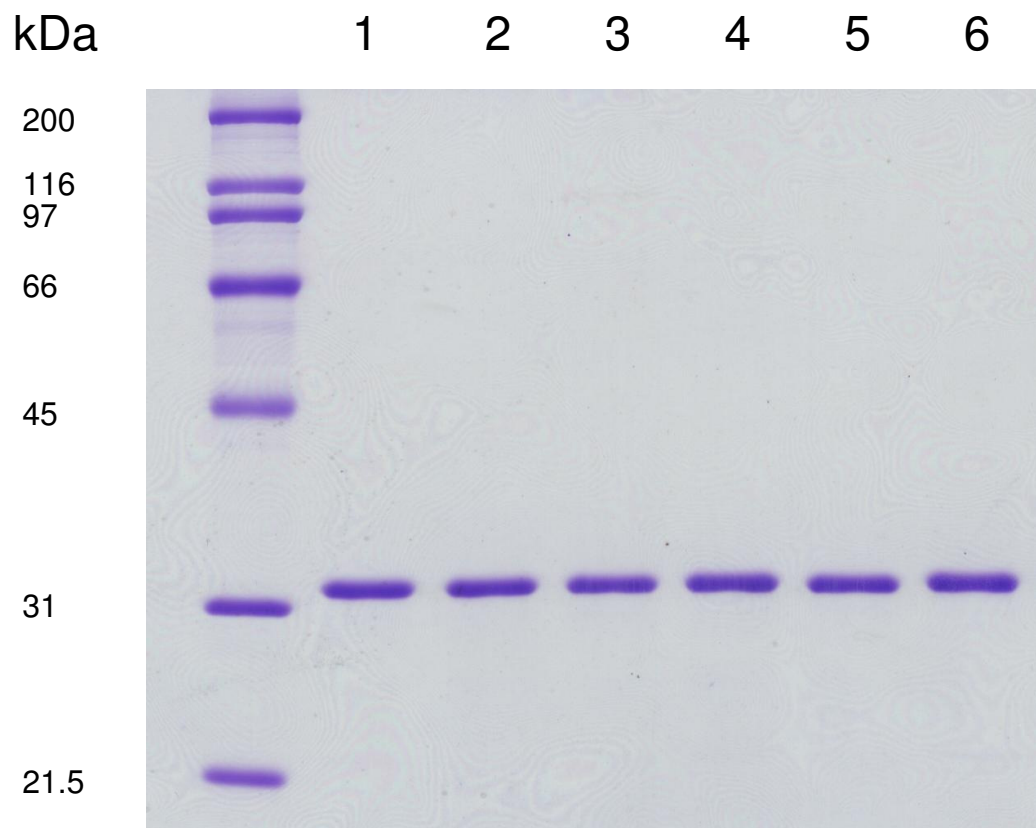
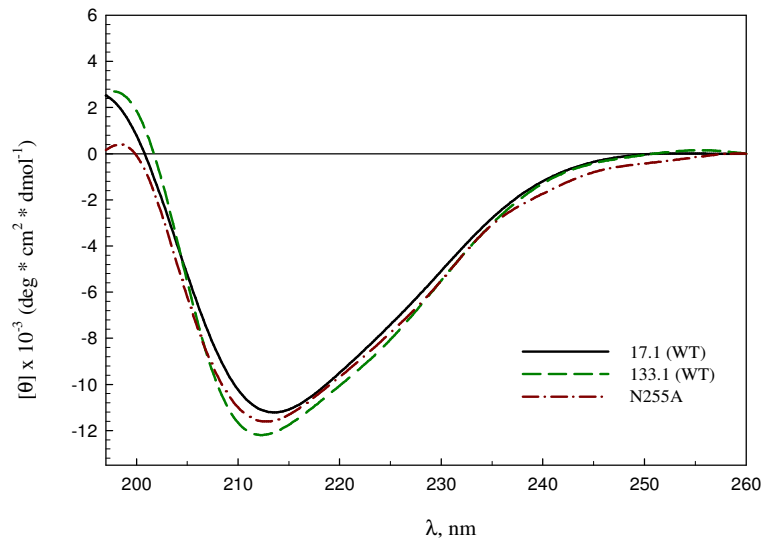


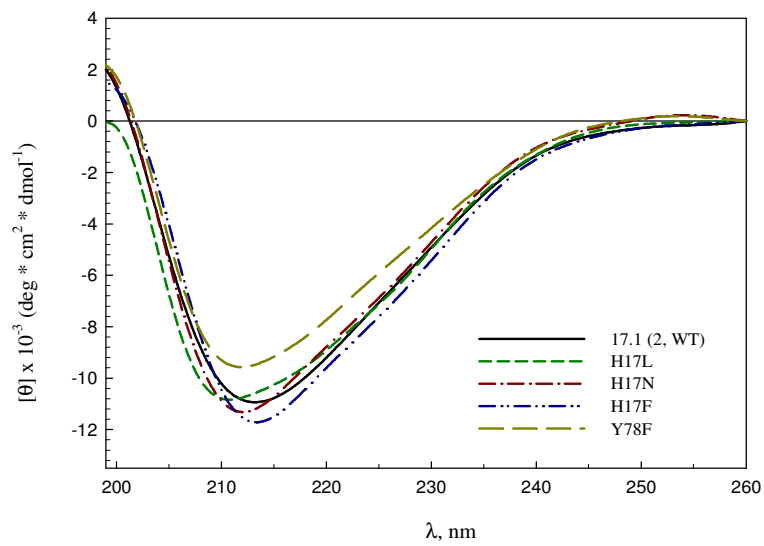
Figure S1

A

CD spectra of WT (17.1 and 133.1) and their mutant analog

**B**

CD spectra of WT 17.1 and its mutant analogs

**Figure S2**

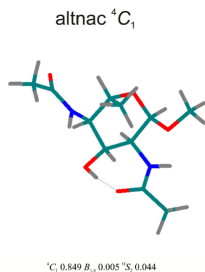
Altnac 4C_1 Conformer

Bond Energy LDA -8.80496866 a.u. Zero-Point Energy : 0.310610 a.u.
 1 a.u. = 2625.4985 kJ mol $^{-1}$ = 627.5095 kcal mol $^{-1}$

Ring Torsion Angles τ_1, τ_2, τ_3 etc Where $\tau_1 = C-1-C-2--C-3-C-4, \tau_2 = C-2-C-3--C-4-C-5$ etc.

-48.50 49.80 -51.17 53.97 -52.78 49.29

Ring Descriptors 1
 4C_1 0.849 $B_{1,4}$ 0.005 5S_1 0.044



Cartesian Coordinates

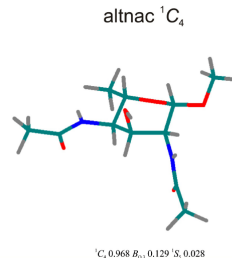
Atom	X	Y	Z (Angstrom)
1 O	0.002366	-0.001222	-0.000915
2 O	6.782206	0.001557	0.000876
3 C	2.866857	3.120294	-0.000004
4 C	2.157558	1.785451	0.146132
5 C	2.814012	0.884273	1.176397
6 C	4.315936	0.813284	0.954004
7 C	4.932218	2.192441	0.812522
8 C	5.088406	2.889487	2.138859
9 H	2.207612	1.271206	-0.832836
10 H	2.632695	1.317122	2.181212
11 H	4.781478	0.337872	1.839559
12 O	4.238260	2.980612	-0.162193
13 H	4.130405	2.993469	2.671677
14 O	2.486731	3.894635	1.107290
15 N	0.774273	2.068607	0.444180
16 O	2.292562	-0.420296	1.078347
17 N	4.541816	-0.016710	-0.197568
18 H	5.929110	2.039175	0.369946
19 H	5.507942	3.895770	1.985294
20 H	5.792581	2.322156	2.768793
21 H	2.524920	3.630917	-0.925578
22 C	2.913640	5.236120	0.993052
23 C	5.762380	-0.432809	-0.548634
24 H	3.731196	-0.596705	-0.447605
25 H	4.015116	5.303813	1.013302
26 H	2.498170	5.788243	1.846174
27 H	2.544778	5.683268	0.409984
28 H	0.591948	3.010752	0.807414
29 C	-0.220682	1.193736	0.294219
30 H	1.381832	-0.352630	0.618767
31 C	-1.603604	1.693325	0.482381
32 C	5.827036	-1.430648	-1.655074
33 H	-2.139052	1.608749	-0.476792
34 H	-1.642316	2.738264	0.820377
35 H	-2.125998	1.047183	1.203119
36 H	6.333711	-0.969838	-2.517538
37 H	4.838903	-1.791974	-1.975442
38 H	6.445480	-2.280835	-1.331032

Altnac 1C_4 Conformer

Bond Energy LDA -8.79841355 a.u. Zero-Point Energy : 0.309077 a.u.

Ring Torsion Angles τ_1, τ_2, τ_3 etc
 51.22 -50.35 55.67 -64.87 67.63 -58.90

Ring Descriptors



Cartesian Coordinates

Atom	X	Y	Z (Angstrom)
1.O	0.070018	-0.039373	-0.016208
2.O	6.213779	-0.028125	0.022546
3.C	2.095308	3.579243	-0.009673
4.C	1.639517	2.173432	-0.301310
5.C	2.671557	1.486981	-1.187159
6.C	4.061002	1.621352	-0.602331
7.C	4.367892	3.071688	-0.246846
8.C	5.687413	3.231252	0.436933
9.H	0.675711	2.186236	-0.840335
10.H	2.404731	0.414978	-1.253498
11.H	4.135891	1.026883	0.326876
12.O	3.354684	3.543358	0.632669
13.H	5.699975	2.652050	1.374740
14.O	1.192095	4.193064	0.824558
15.N	1.462872	1.456201	0.924271
16.O	2.710164	2.077680	-2.472877
17.N	5.001382	1.076687	-1.531094
18.H	4.338817	3.674730	-1.181684
19.H	5.878430	4.291670	0.660588
20.H	6.497141	2.853044	-0.206338
21.H	2.204226	4.136085	-0.971030
22.C	1.486537	5.565191	1.011861
23.C	6.003745	0.256558	-1.160396
24.H	4.811753	1.248703	-2.522064
25.H	2.463340	5.696120	1.506603
26.H	0.692630	5.985411	1.642772
27.H	1.499920	6.092931	0.039331
28.H	1.926456	1.815130	1.762095
29.C	0.659739	0.379733	0.987181
30.H	1.950791	1.747721	-2.992212
31.C	0.526645	-0.272144	2.320310
32.C	6.847299	-0.282421	-2.265552
33.H	1.114893	0.220753	3.108074
34.H	0.844098	-1.322584	2.234556
35.H	-0.535533	-0.276278	2.608849
36.H	7.891981	0.018996	-2.094490
37.H	6.531500	0.056313	-3.263193
38.H	6.817139	-1.382069	-2.228743

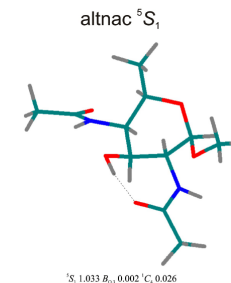
Altnac 5S_1 Conformer

Bond Energy LDA -8.80274347 a.u. Zero-Point Energy : 0.309753 a.u.

Ring Torsion Angles τ_1, τ_2, τ_3 etc
 -27.84 -30.93 64.31 -32.52 -28.90 61.50

Ring Descriptors

5S_1 1.033 $B_{0,3}$ 0.002 1C_4 0.026



Cartesian Coordinates

Atom	X	Y	Z (Angstrom)
1.O	0.290764	-0.136407	-0.454159
2.O	7.147550	0.772904	-0.573867
3.C	2.802110	3.178211	0.384314
4.C	2.090093	1.956874	-0.133606
5.C	3.087804	0.831148	-0.429526
6.C	4.450171	1.404800	-0.783658
7.C	4.289387	2.750036	-1.467066
8.C	5.584671	3.338114	-1.927545
9.H	1.618809	2.220988	-1.098647
10.H	3.187143	0.209020	0.483282
11.H	5.043374	1.573410	0.132563
12.O	3.704228	3.684611	-0.551451
13.H	6.034409	2.698803	-2.703910
14.O	3.402280	2.800808	1.593076
15.N	1.066357	1.573265	0.799942
16.O	2.623700	0.058123	-1.512318
17.N	5.149178	0.449480	-1.582952
18.H	3.600273	2.625030	-2.330397
19.H	6.290131	3.406259	-1.083397
20.H	5.419423	4.340655	-2.351009
21.H	2.089173	4.007602	0.586047
22.C	4.021167	3.892656	2.241692
23.C	6.448835	0.157096	-1.385254
24.H	4.555614	-0.153531	-2.161797
25.H	3.292891	4.708893	2.414193
26.H	4.860309	4.283598	1.640595
27.H	4.397307	3.531195	3.207626
28.H	1.075819	2.020053	1.720170
29.C	0.226148	0.559548	0.581369
30.H	1.652420	-0.114852	-1.260960
31.C	-0.803194	0.296587	1.616689
32.C	6.997859	-0.953715	-2.215905
33.H	-1.798277	0.429725	1.163912
34.H	-0.716281	0.957318	2.490623
35.H	-0.730064	-0.753533	1.936919
36.H	7.826803	-0.564573	-2.826761
37.H	6.249954	-1.417065	-2.875924
38.H	7.419743	-1.719862	-1.547688

Figure S3

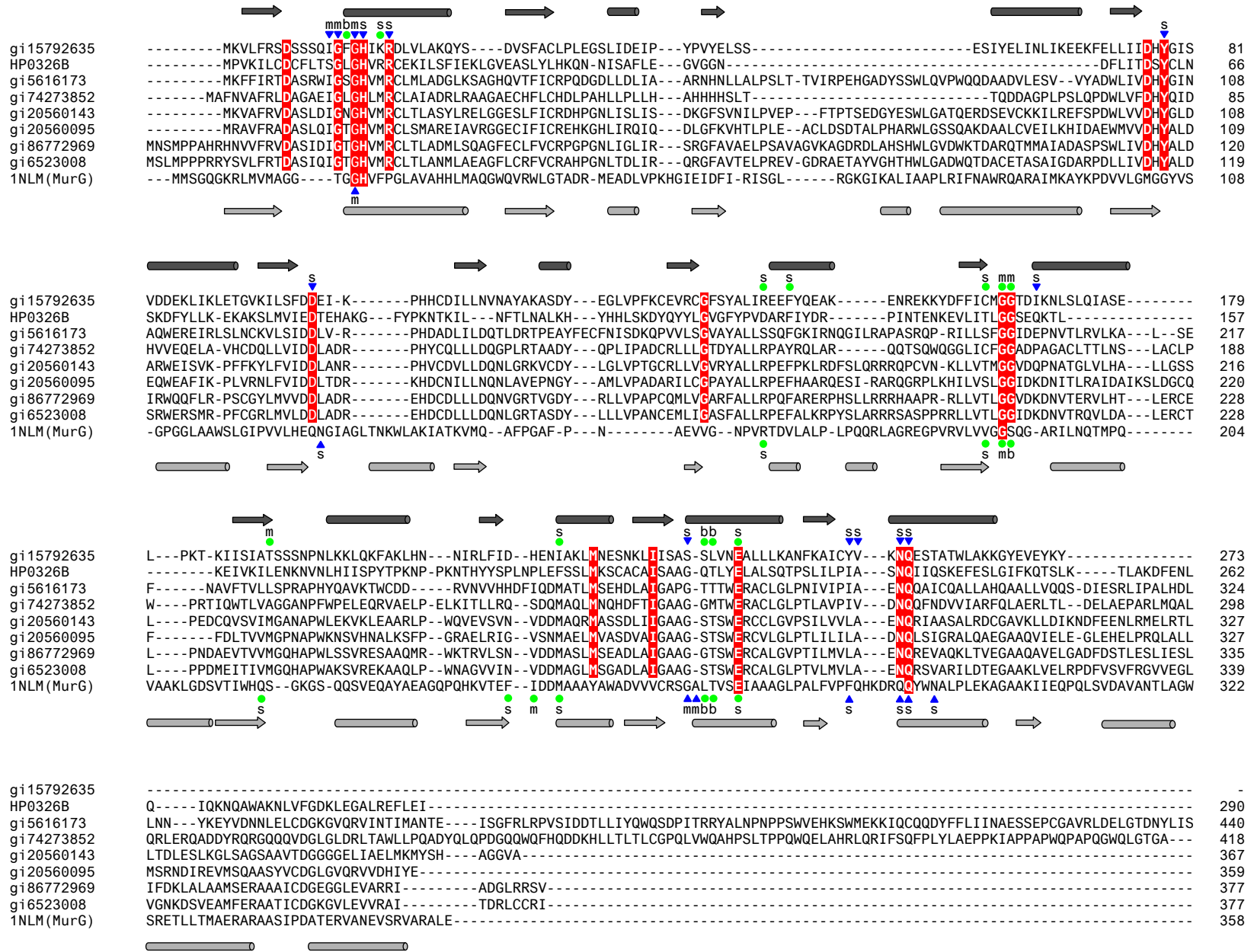
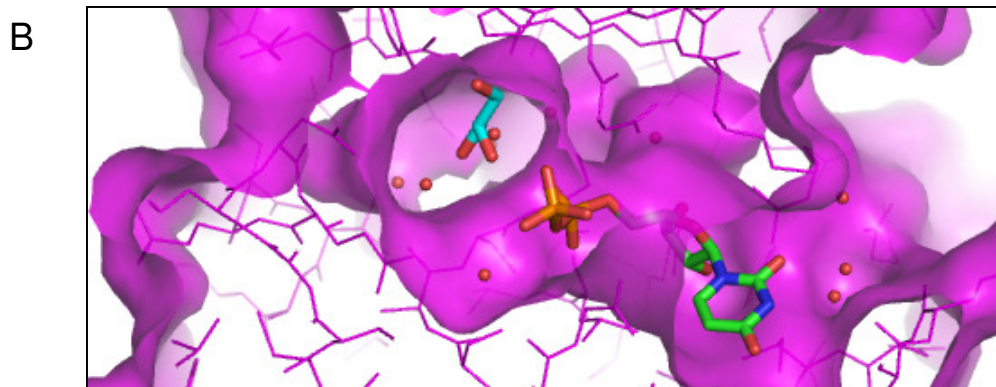
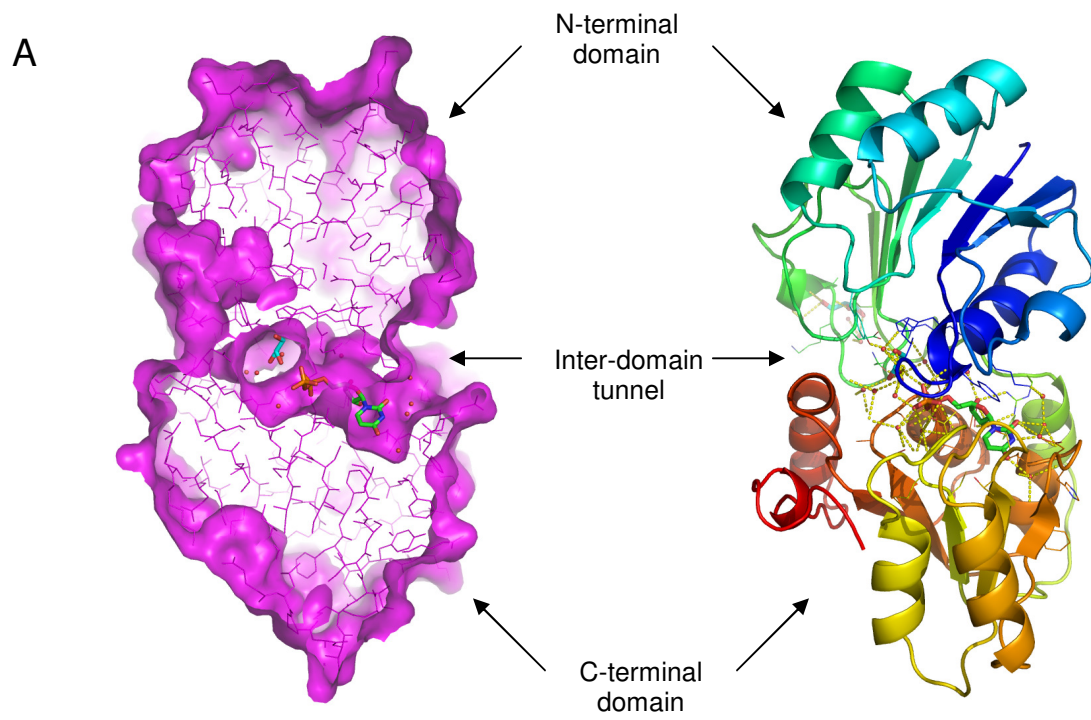


Figure S4



C

Detailed description: Panel C is another close-up view of the inter-domain tunnel region, showing the protein backbone in magenta and side chains in various colors. This view is oriented differently from panel B, providing a different perspective of the tunnel's interior and the arrangement of the side chains. The tunnel appears to be a well-defined pocket for a ligand.

Figure S5

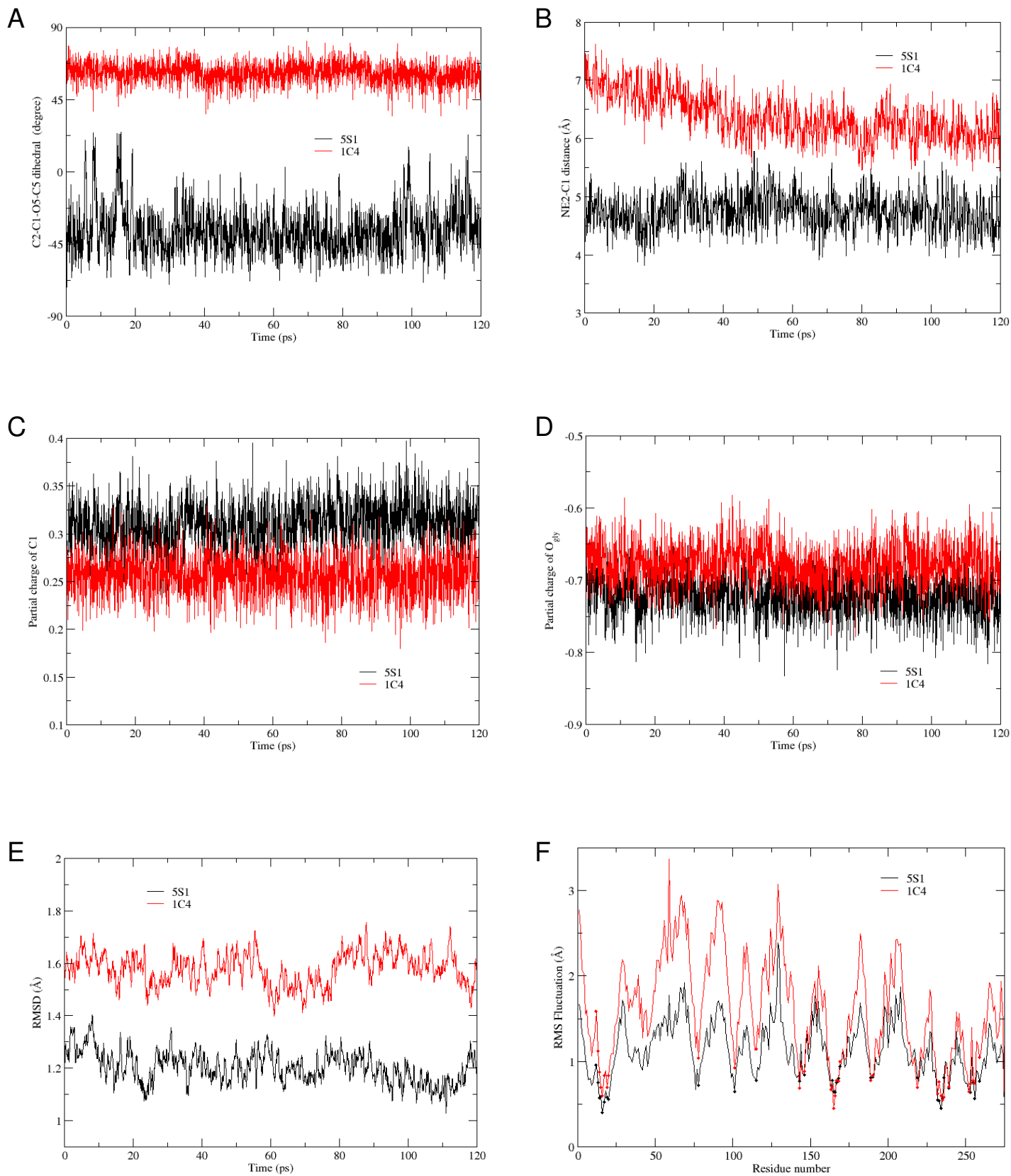


Figure S6

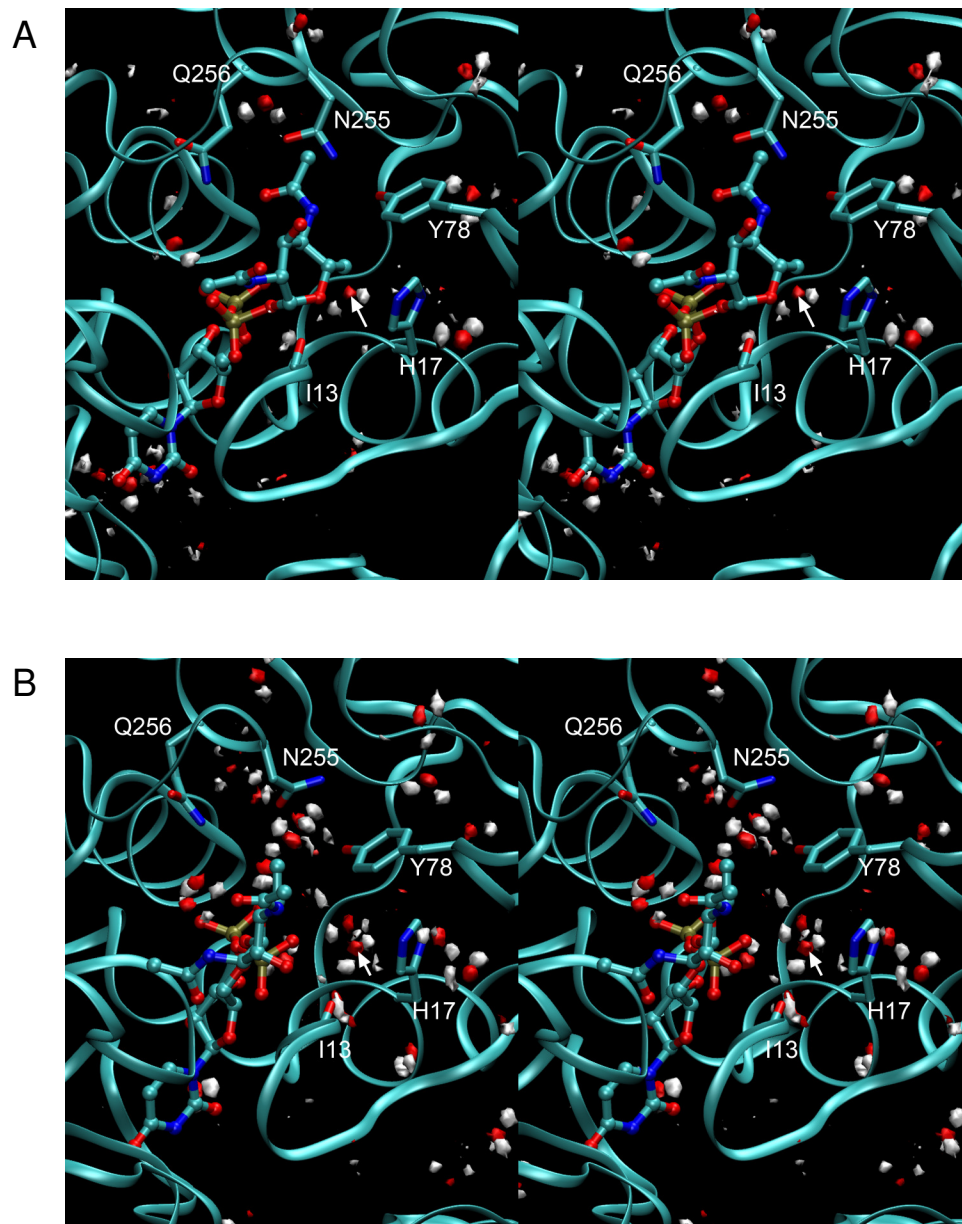


Figure S7

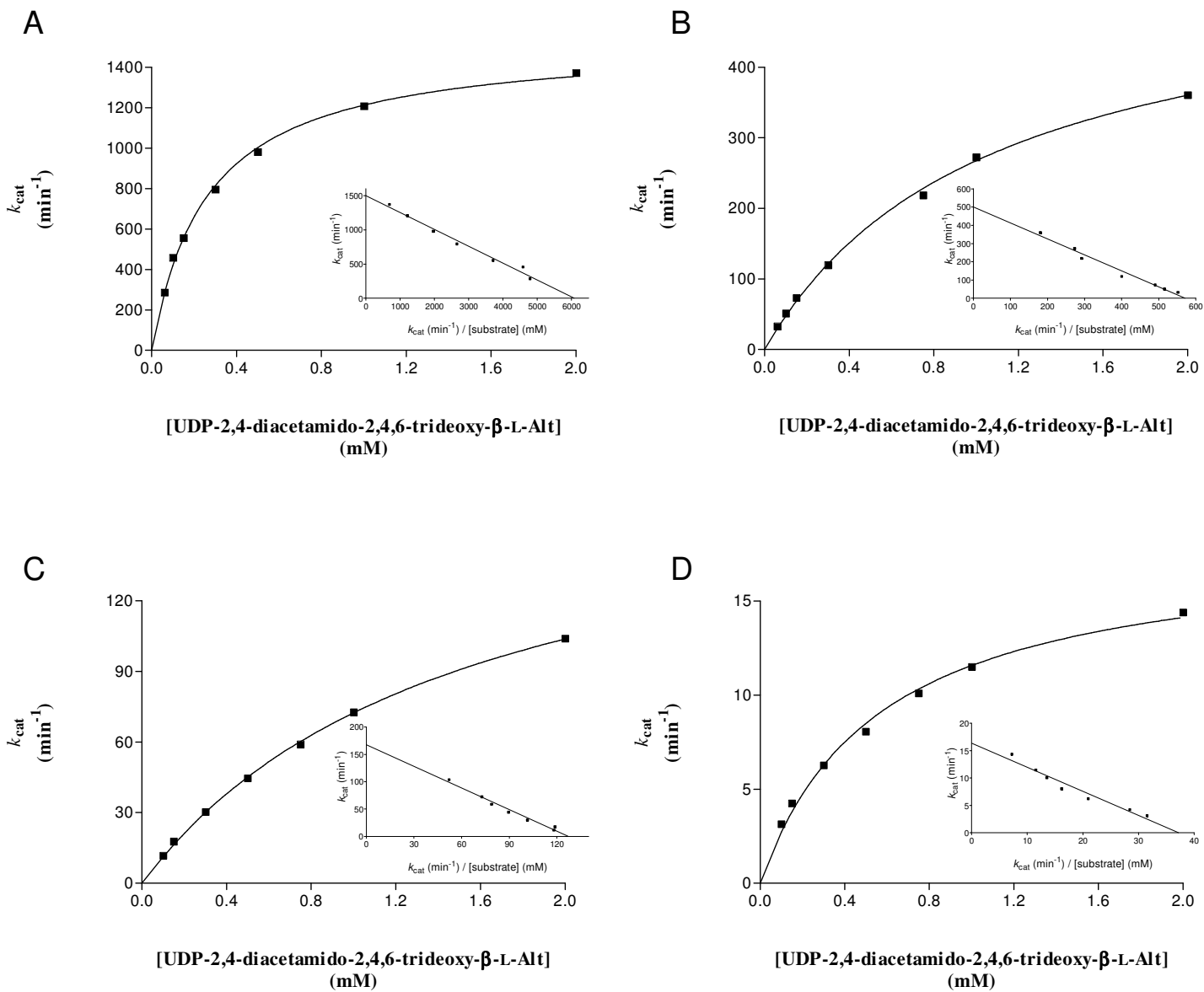


Figure S8

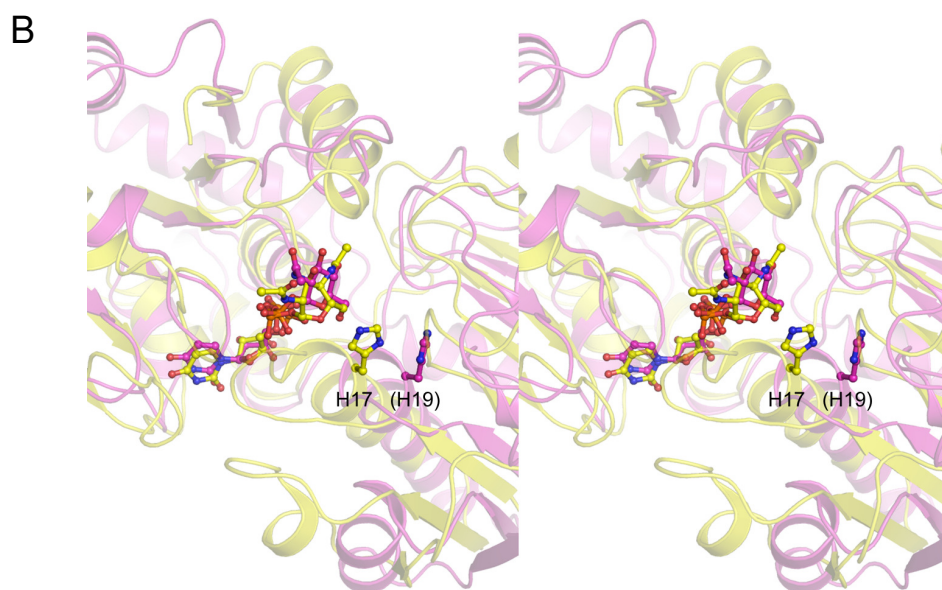
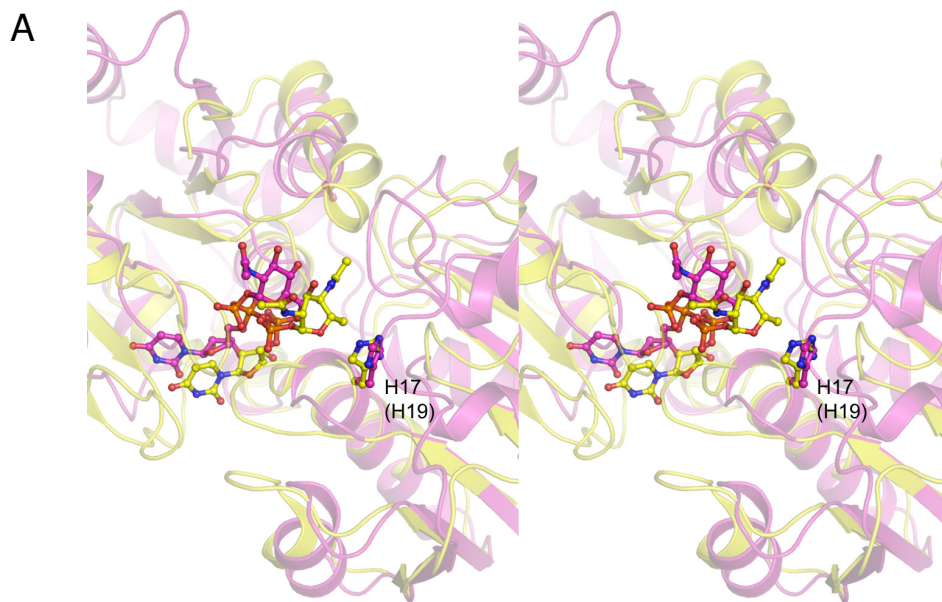


Figure S9